

## Article

# Numerical Assessment and Parametric Optimization of a Piezoelectric Wind Energy Harvester for IoT-Based Applications

Muhammad Abdullah Sheeraz <sup>1</sup>, Muhammad Sohail Malik <sup>1</sup>, Khalid Rehman <sup>1</sup>, Hassan Elahi <sup>2,\*</sup>, Zubair Butt <sup>3</sup>, Iftikhar Ahmad <sup>4</sup>, Marco Eugeni <sup>2</sup> and Paolo Gaudenzi <sup>2</sup>

<sup>1</sup> Faculty of Mechanical Engineering, GIK Institute of Engineering Sciences and Technology, Topi 23460, Pakistan; abdullahtlg8@gmail.com (M.A.S.); sohailmalik49@gmail.com (M.S.M.); khalid.rehman@giki.edu.pk (K.R.)

<sup>2</sup> Department of Mechanical and Aerospace Engineering, Sapienza University of Rome, Via Eudossiana 18, 00184 Rome, Italy; marco.eugeni@uniroma1.it (M.E.); paolo.gaudenzi@uniroma1.it (P.G.)

<sup>3</sup> Department of Mechanical Engineering, University of Engineering and Technology Taxila 47080, Pakistan; zubair.butt@uettaxila.edu.pk

<sup>4</sup> Department of Mechanical Engineering, School of Engineering Bahrain Polytechnic, Isa Town P.O. Box 33349, Bahrain; iftikhar.ahmad@polytechnic.bh

\* Correspondence: hassan.elahi@uniroma1.it



**Citation:** Sheeraz, M.A.; Malik, M.S.; Rehman, K.; Elahi, H.; Butt, Z.; Ahmad, I.; Eugeni, M.; Gaudenzi, P. Numerical Assessment and Parametric Optimization of a Piezoelectric Wind Energy Harvester for IoT-Based Applications. *Energies* **2021**, *14*, 2498. <https://doi.org/10.3390/en14092498>

Academic Editor:  
Abdessattar Abdelkefi

Received: 1 April 2021  
Accepted: 24 April 2021  
Published: 27 April 2021

**Publisher's Note:** MDPI stays neutral with regard to jurisdictional claims in published maps and institutional affiliations.



**Copyright:** © 2021 by the authors. Licensee MDPI, Basel, Switzerland. This article is an open access article distributed under the terms and conditions of the Creative Commons Attribution (CC BY) license (<https://creativecommons.org/licenses/by/4.0/>).

**Abstract:** In the 21st century, researchers have been showing keen interest in the areas of wireless networking and internet of things (IoT) devices. Conventionally, batteries have been used to power these networks; however, due to the limited lifespan of batteries and with the recent advancements in piezoelectric technology, there is a dramatic increase in renewable energy harvesting devices. In this research, an eco-friendly wind energy harvesting device based on the piezoelectric technique is analytically modeled, numerically simulated, and statistically optimized for low power applications. MATLAB toolbox SIMSCAPE is utilized to simulate the proposed wind energy harvester in which a windmill is used to produce rotational motion due to the kinetic energy of wind. The windmill's rotational shaft is further connected to the rotary to linear converter (RLC) and vibration enhancement mechanism (VEM) for the generation of translational mechanical vibration. Consequently, due to these alternative linear vibrations, the piezoelectric stack produces sufficient electrical output. The output response of the energy harvester is analyzed for the various conditions of piezoelectric thickness, wind speed, rotor angular velocity, and VEM stiffness. It is observed that the electrical power of the proposed harvester is proportional to the cube of wind speed and is inversely proportional to the number of rotor blades. Furthermore, an optimization strategy based on the full factorial design of the experiment is developed and implemented on MINITAB 18.0 for evaluating the statistical performance of the proposed harvester. It is noticed that a design with 3 rotor-blades, having 3 mm piezoelectric thickness, and 40 Nm<sup>-1</sup> stiffness generates the optimum electrical response of the harvester.

**Keywords:** energy harvesting; piezoelectric transducers; vibration enhancement mechanism (VEM); design of experiments-based optimization; internet of things (IoT)

## 1. Introduction

During the past few years, researchers have been trying to explore the area of energy harvesting system which is the process used to obtain electrical energy from the natural resources available in the environment. In other words, this process is based on renewable sources that are replenished on a human timescale such as mechanical vibration, solar radiations, hydropower, wind energy, thermoelectricity, and physical motions [1–5]. Nowadays, wind energy is one of the prominent green sources to solve the energy crisis and environmental pollution [6]. It has been observed that wind turbines are extensively used to produce electrical energy from the wind forces present in an ambient environment.

However, examining the characteristics of energy sources without considering the impact they have on the environment is not conceivable. Over time and due to the variation of wind forces with non-typical loads may result in the structural failure of wind energy harvesters [7,8]. Moreover, the structure of large-size wind turbines is complex and there is always an imperious need to minimize the cogging torque for smooth and cut-in operations [9]. The distribution of defects in the blades of wind energy harvester is also increasing day by day which in turn reduces the effectiveness and efficiency of the harvester. Researchers evidenced that one error in the design of an energy harvester can trigger several unacceptable errors. Therefore, the performance of each component plays a noteworthy role in the generation of electrical energy [10,11]. Furthermore, over the decades, many conventional and unconventional approaches are on the way up to harvest electrical energy. These approaches are mainly based on renewable and non-renewable energy sources; h adverse issues, researchers are considering the alternative energy approach to harvest cost-effective electrical energy [12,13]. Additionally, in the recent past, several techniques are also introduced to convert wind forces into a reliable form of vibrations, which can be utilized to produce sufficient voltage. These techniques have also opened a new research area of harvesting wind energy using the mechanical vibration caused by wind forces [14]. From the literature, it has been noticed that due to the highly efficient output and low-cost nature of piezoelectric materials, piezoelectric transduction is the prominent candidate for generating electrical energy [15–17]. It is interesting to note that the pyroelectric effect is a fundamental concept behind piezoelectricity. In the mid-eighteenth century, pyroelectricity was proposed to predict the reaction of piezoelectric materials with the variation in the temperature. Drawing on this information, a connection between mechanical pressure and the electric charge has been justified which in turn gives us the required piezoelectric effect [18,19]. Piezoelectric materials are capable of producing alternating voltage when they are excited by mechanical vibration [20]. On the contrary, when the electric field is applied to these materials, they show mechanical strain or vibration, and various categories of piezoelectric effect [21,22] are shown in Figure 1.

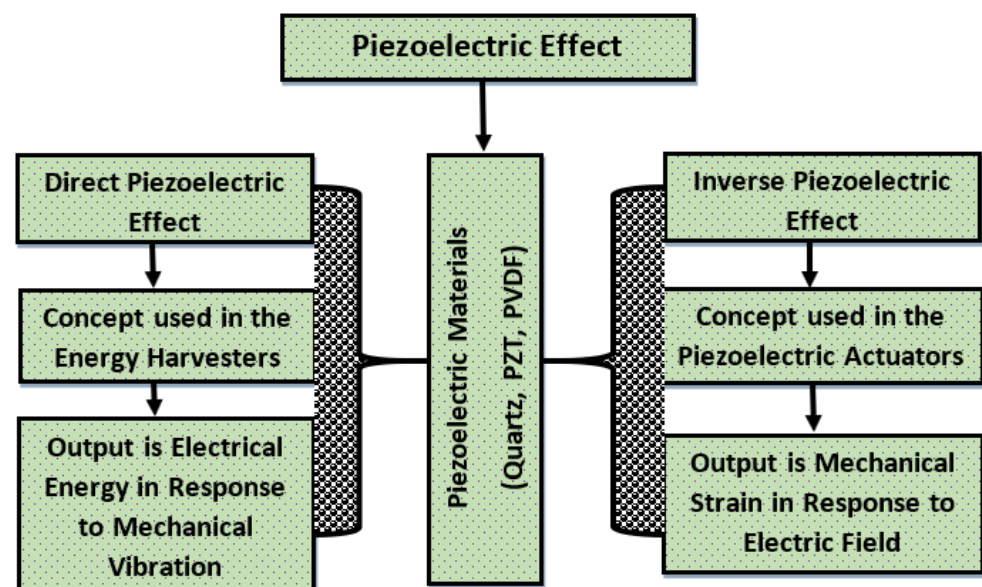


**Figure 1.** Categories of the piezoelectric effect.

Even nowadays, piezoelectric materials are being utilized in the development of cost-effective, durable, and efficient wind energy harvesters. Researchers have designed and developed a wind energy harvester based on the Lead Zirconate Titanate (PZT) material being fixed in the inverted flag orientation. It is observed that the geometry of the flag plays a vital role in determining the electrical response of the harvester. Therefore, a self-alignment mechanism has been introduced to tune the geometrical properties of the

PZT sensor and the harvester is capable of producing a power of 5 mW in response to  $9 \text{ ms}^{-1}$  wind speed [23]. In the recent past, the design of an energy harvester based on PZT-Stack has been proposed to observe the voltage-power characteristics of a piezoelectric transducer. A transition system is also noticed, which was used to transfer the mechanical vibration from the industrial machine to PZT-Stack and the harvester is capable of producing a voltage of 3.85 V [24]. Moreover, for the last few years, researchers have been developing optimized vibrational scavengers for harvesting wind energy. A mathematical model of the cantilever-based harvester is studied to analyze the interrelationships between piezoelectric voltage and parameters of wind energy. The influence of change in length and location of piezo patches on the harvester's output is also observed. It is noticed that the output response of the harvester is maximum only when the resonant frequency of a cantilever matches the vortex shedding frequency. Furthermore, 1.02 W power is practically observed with the variation in the wind velocity ranging from  $9\text{--}10 \text{ ms}^{-1}$  [25]. Theoretical analysis based on ten bimorph sensors has been investigated to observe the generated electrical energy from a prototype of the wind energy harvester. Interestingly, the harvester can produce sufficient energy even at a frequency range less than the resonant frequency of bimorph materials. A comparison between analytical and experimental design has been carried out, and 7.5 mW power is noticed at a wind speed of  $4.47 \text{ ms}^{-1}$  [26]. An analytical model of the novel piezoelectric energy harvester is studied to investigate the electrical response after the flutter velocity. The designed harvester works on the non-linear aerodynamics' principle, and thus, generated electrical energy is due to the excitations produced by limit cycle oscillations (LCOs). Additionally, the authors have checked the efficiency of the harvester by considering two different PZT materials; PZT-5A and Barium Titanate ( $\text{BaTiO}_3$ ). It is observed that the harvester based on PZT-5A generates more electrical output as compared to  $\text{BaTiO}_3$  [27]. The performance of piezoelectric wind energy harvesters is highly dependent on the conversion of aerodynamic forces into accelerated mechanical vibrations. Therefore, a piezoelectric wind energy harvester based on the bluff body has been developed in which a transition from vortex-induced vibration to galloping is done by Y-shaped attachments. It is observed that the attachment of y-structures to the bluff body increases the amplitude of mechanical vibration. Consequently, the designed harvester produces sufficient electrical energy even at low wind speeds [28]. Zhang et al., utilized a concept of nonlinear magnetic forces to increase the output response of the energy harvester based on the vortex-induced vibrations. Interestingly, the authors have investigated the effect of the relative distance between the magnets on the natural frequency of the harvester [29]. The conversion of aerodynamic forces into a reliable form of electrical energy is highly dependent on a particular category of the energy harvester [30]. Therefore, in one of the articles, researchers have modeled torsional-flutter wind energy harvester and correspondingly analyzed the electrical efficiency by tuning the electromechanical nature of the harvester. Based on the outcomes, the authors have recommended utilizing this harvester for low-power applications [31]. Similarly, Elahi et al., worked on various mechanisms for the transformation of airflow into useful electrical energy by using piezoelectric sensors having applications in the field of structural health monitoring and self-powered IoT devices [32–34]. The concept of fluttering plays a vital role in determining the effectiveness of wind energy harvesters. Therefore, researchers have been trying to design and develop wind energy harvesters based on the flutter phenomenon [35,36]. A concept of fluid-structure interaction (FSI) is also getting popular in the designing of piezoelectric energy harvesters. Elahi et al. presented a cantilever-flag-based piezoelectric energy harvester that was analyzed by considering the PZT and aluminum (Al) patches to check the stability of the harvester. The design was simulated on MSC Nastran and the performance of the harvester was experimentally evaluated by varying the resistive load. The maximum electrical power was found to be 1.12 mW at an optimal resistive load of  $66.6 \text{ k}\Omega$  [37]. Elvin et al. proposed a novel approach to analyze the fluctuations in the flutter speed and output voltage of the harvester for a passive PZT damping at time-variant loading conditions. It is observed that the open circuit stiffness increases the flutter speed of

the designed harvester. Furthermore, the authors have justified that the electromechanical coupling coefficient plays a noteworthy role in determining the range of flapping behavior and is having a direct relationship to the electrical energy of the harvester [38]. Bae et al., analyzed the performance of a two-degree of freedom (DOF) wind energy harvester based on the piezoelectric technique. It is contemplated that the pitch-to-plunge and frequency ratios are the two important variables in acquiring the effective power density from a non-linear wind energy harvester. The authors demonstrated that linear wind energy harvester can generate electrical energy only in the range of flutter velocity. On the contrary, LCOs are obtained for a nonlinear energy harvester which in turn force the PZT material to generate sufficient voltage [39]. A novel approach to harvest wind energy is analyzed in which the turbine operates at a low Reynold's number ( $2 \times 10^4$ ) and an acceptable power coefficient is observed at the tip speed ratio of 0.7 [40]. Several optimization techniques are also investigated to improve the efficiency of the energy harvester [41,42]. One such method is based on optimizing the geometry of a cantilever beam, which is excited by lateral force to study different distributions of PZT layers. Finite element analysis (FEA) has been carried out on Ansys, and the verified model is also used to calculate the dissipated energy due to relative distributions of PZT beams [43]. Normally, the output response of the energy harvester does not produce enough voltage necessary to drive a wireless network. Therefore, the power quality enhancement circuit is also reported in the article in which authors have presented the static multicell converters to enhance and stabilize the electrical energy of wind energy harvesters [44]. Moreover, observations from the literature reveal that by minimizing the capacitive load on the PZT materials, the output response could be enhanced up to 95% as compared to energy obtained from conventional full-bridge rectifiers [45].

In this research work, a wind energy harvesting model based on piezoelectric transduction is presented. An analytical model of the harvester has been discussed and enhanced by implying the influence of PZT thickness on the electrical response of wind energy harvester. In the proposed energy harvester, a windmill is used to generate the rotational motion due to the kinetic energy of the wind. The windmill's shaft is further connected to the wheel of RLC to obtain alternative mechanical vibration for PZT-Stack. The amplitude of translational mechanical vibrations has been increased by utilizing the VEM of an appropriate stiffness. Furthermore, MATLAB toolbox SIMSCAPE is utilized to simulate the proposed design and analyze the impact of wind speed, stiffness of VEM, PZT thickness, and the number of rotor-blades on the electrical response of the energy harvester. A literature review shows that researchers have been trying to optimize the electrical output of renewable energy systems. Therefore, the Full factorial design of the experiment (DOE) is performed on MINITAB 18.0 (Version 18.0; Pennsylvania) to optimize the parameters of the proposed energy harvesting system. Furthermore, simulation outcomes are well-verified with the optimization and literature results of wind energy harvesters. Section 2 of the manuscript presents the theoretical model of the harvester; Section 3 explains the numerical analysis of the proposed harvester; Section 4 elaborates the optimization strategy for the proposed harvester; a campaign of simulation and optimizations results is carried out in Section 5.

## 2. Analytical Model

The schematic of the proposed energy harvester is shown in Figure 2 in which a windmill is used to extract the rotational kinetic energy from wind present in the ambient environment. However, for the energy harvesters based on piezoelectric transductions, translational mechanical vibration is needed to acquire useful electrical output. Therefore, the output shaft of the windmill is further connected to the wheel of RLC for the generation of linear motion. This mechanism consists of a slotted rod and a cylindrical slider (scotch yoke mechanism) to make sure that the predefined motion is only in the direction perpendicular to the axis of the shaft.

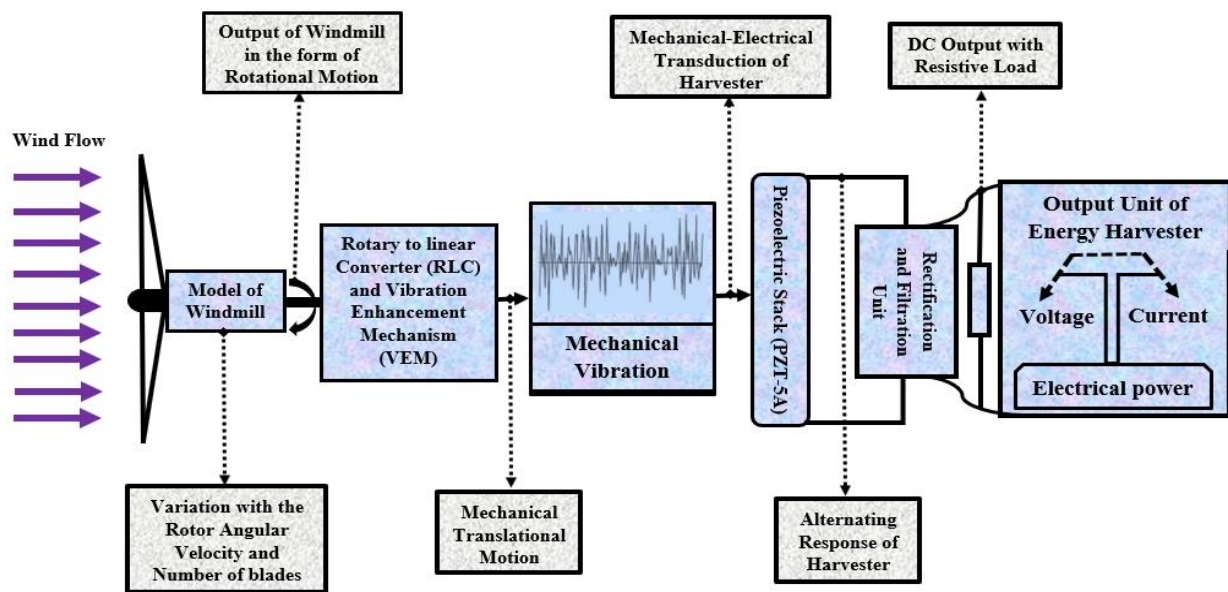


Figure 2. Schematic of the proposed piezoelectric wind energy harvester.

Linear movement obtained from this mechanism depends upon the distance between the slider and slotted rod ( $Z$ ), so, the endpoints of the slotted rod are linearly displaced by  $Z_s$  as given in Equation (1).

$$Z_s = Z \sin \omega t \quad (1)$$

It has been observed that mechanical vibrations produced from RLC are not enough for piezoelectric materials to produce a useful electrical output. Therefore, a VEM has been used to enhance the amplitude of alternative mechanical vibration. Qian et al., presented the optimal force frame for PZT-Stack in which translational motion has been obtained by utilizing the beam of a particular Young's modulus ( $E_B$ ) [46]. Besides that, in the recent past, J.X Tao and Q. Wang developed an analytical model for the piezoelectric wind energy harvester [47]. Therefore, in this research work, VEM is considered as a lever mechanism whose one end is fixed which is further divided into short and long moment arms denoted by ' $L_s$ ' and ' $L_l$ ' respectively. Additionally, it is also noticed that only harmonic motion is obtained by using RLC; therefore, it is necessary to utilize a combination of Hookean springs to attain useful mechanical vibration for the piezoelectric stack. Literature studies reveal that proof mass has a prominent role in displacing the structure to produce deformations in the piezoelectric materials. Researchers have already analyzed the piezoelectric energy harvester by varying the geometrical features of the proof mass. Therefore, in this research work, stiffness of VEM has been considered to analyze the performance of the piezoelectric wind energy harvester as shown in Figure 3. Furthermore, the magnifying ratio as given in Equation (2) plays a prominent role in the enhancement of alternative mechanical vibration for PZT-Stack.

$$\eta_m = \frac{L_l}{L_s} \quad (2)$$

However, for simplification, in this research work, only the stiffness of the mechanism has been considered as a variable to numerically investigate the response of the proposed harvester. Therefore, equivalent mass distribution for PZT-Stack is highly dependent on the rotor-area, air-density, blade-length, and magnifying ratio as given in Equation (3).

$$m_e = \rho A L_b \eta_m \quad (3)$$

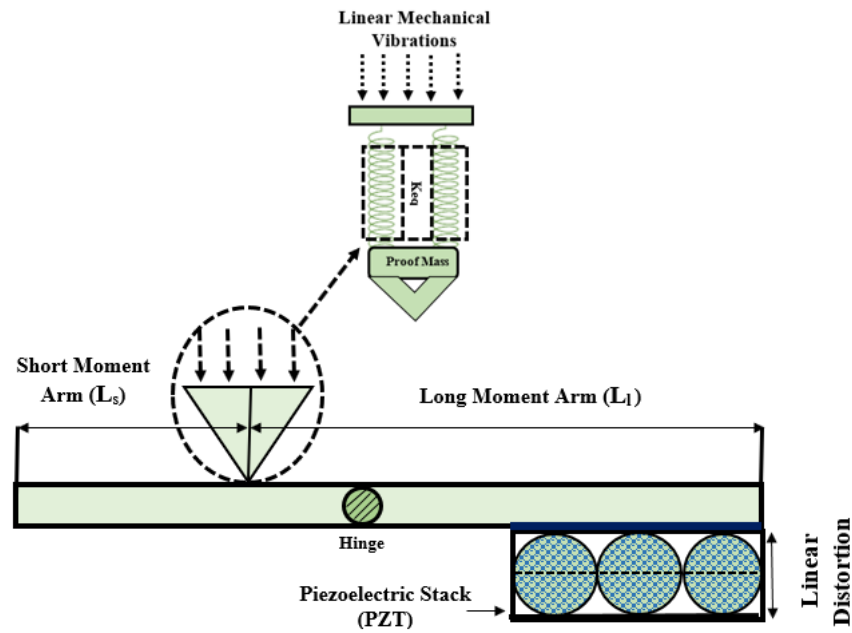


Figure 3. Analysis of mechanical vibration via conceptual design of VEM.

In the proposed energy harvester model, stiffness of both PZT-Stack and VEM plays a vital role in determining the electrical response of the energy harvester as given in Equations (4) and (5).

$$K_b = \frac{E_b a h^3}{4L_l^3} \quad (4)$$

$$K_p = \frac{E_p w_p}{\eta_m^2} \quad (5)$$

where  $E_p$  and  $w_p$  are Young's modulus and width of a PZT material. Furthermore, equivalent stiffness ( $K_e$ ) is obtained by considering a parallel combination of VEM and PZT-Stack. Finally, the equation of motion for the proposed piezoelectric wind energy harvester is obtained using Newton's second law of motion, as given in Equation (6).

$$m_e \ddot{Z}_e + C \dot{Z}_e + K_b Z_e = F(\sin \omega t) \quad (6)$$

In Equation (6),  $\dot{Z}_e$  is the equivalent mass displacement that mainly depends upon the amplitude and the phase angle of the mechanical vibration. Hence, the equivalent force being applied to PZT-Stack ( $F_p$ ) is highly dependent on the magnifying ratio, equivalent displacement, and the damping force as given in Equation (7).

$$F_p = \eta_m (K_b Z_e(t) - C \dot{Z}_e(t)) \quad (7)$$

Due to the application of alternative load on PZT-Stack, the polarization effect is influenced, and an electric charge is generated at the electrode as given in Equation (8). Moreover, the parametric relationship between capacitor and voltage is used to obtain the desired equation for the generated voltage, as given in Equation (9).

$$Q = d_{33} \eta_m (K_b Z_e(t) - C \dot{Z}_e(t)) \quad (8)$$

$$V = \frac{d_{33} \eta_m (K_b Z_e(t) - C \dot{Z}_e(t))}{C_p} \quad (9)$$

In Equation (9),  $C_p$  is the piezoelectric capacitance, which is the function of vacuum permittivity, relative dielectric permittivity, length, width, and thickness of the piezo-

electric stack ( $C_p = \frac{\epsilon_r \epsilon_0 \omega_p L_p}{t_p}$ ). Therefore, final expressions for the generated voltage and current of wind energy harvester based on the piezoelectric technique are given in Equations (10) and (11).

$$V = \frac{d_{33} \eta_m (K_b Z_e(t) - C \dot{Z}_e(t)) t_p}{\epsilon_r \epsilon_0 \omega_p L_p} \quad (10)$$

$$I = \frac{d_{33} \eta_m (K_b Z_e(t) - C \dot{Z}_e(t)) t_p}{\epsilon_r \epsilon_0 \omega_p L_p R} \quad (11)$$

### 3. Simulation and Analysis

MATLAB is a programming package containing various modules and built-in functions to analyze the performance of realistic systems. MATLAB toolbox SIMSCAPE can design, simulate, and evaluate the output response of the engineering systems by considering different independent variables. Therefore, the proposed piezoelectric wind energy harvester has been designed, simulated, and analyzed under the predefined levels of the input parameters. A horizontal axis windmill has been modeled by utilizing the optimal condition of the tip-speed ratio that mainly depends upon the number of the rotor-blades. Figure 4 shows that a rotational motion sensor is utilized in the Simscape environment to analyze the rotor angular velocity under the time-variant wind-speed, and the number of rotor-blades.

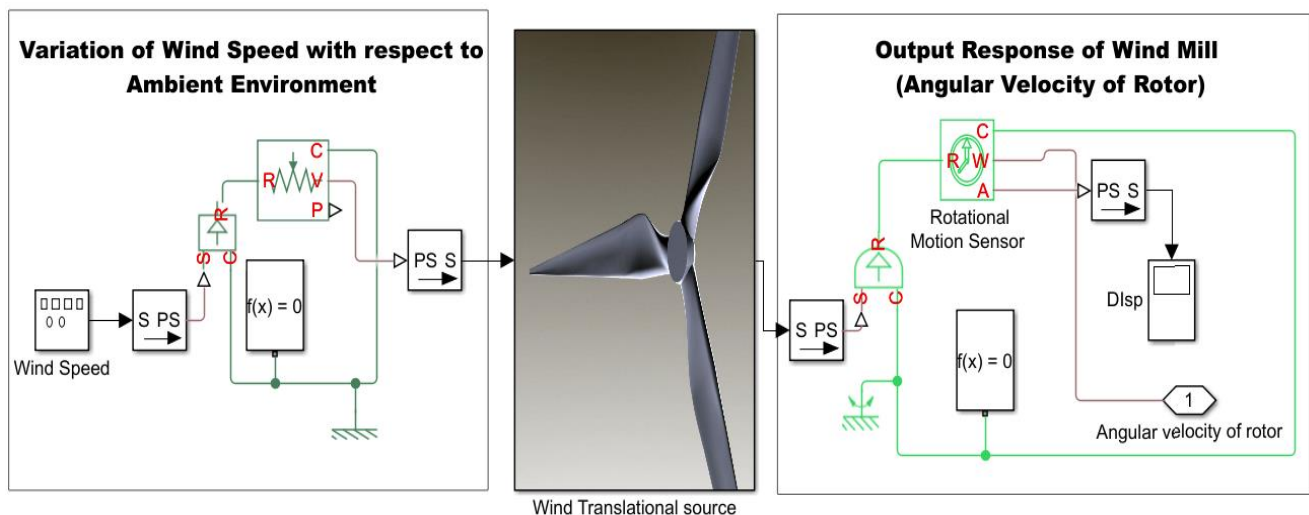
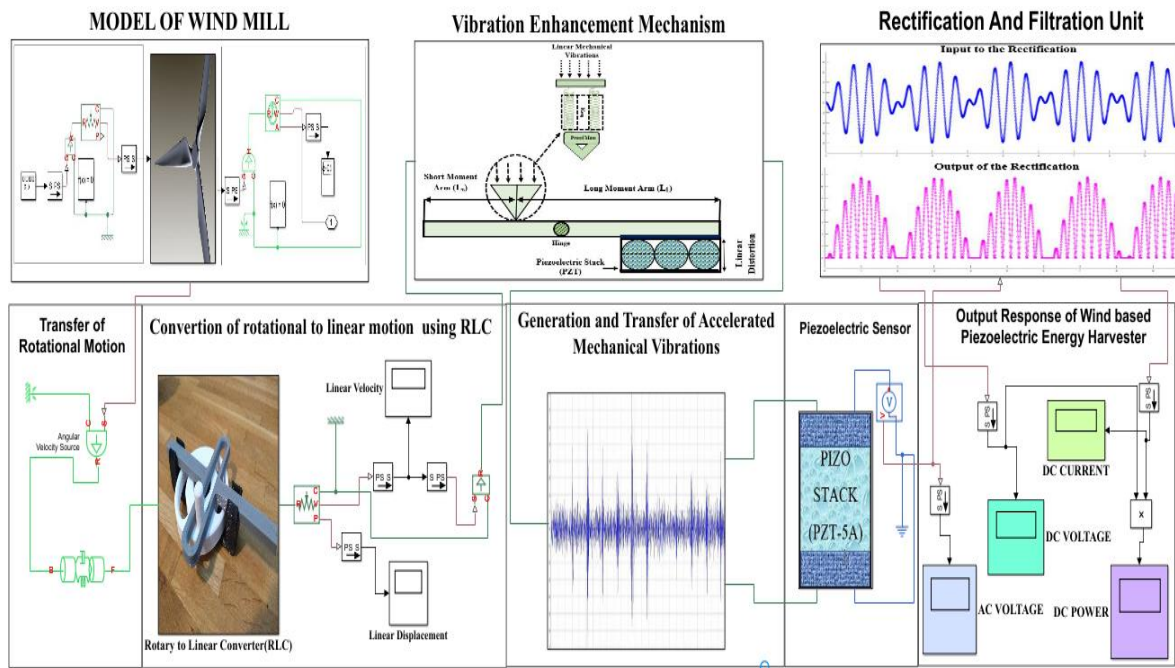


Figure 4. Model of windmill on SIMSCAPE.

For piezoelectric transduction, it is necessary to convert this rotational motion into translational motion. Therefore, the output shaft of the windmill is further connected to the RLC for the generation of alternative mechanical vibration sensed by a translational motion sensor. A VEM which is a combination of Hookean springs and proof mass has been utilized to increase the amplitude of linear vibration. The structure of VEM contains the parallel combination of springs; therefore, cumulative force, in this case, will be the sum of two forces generated due to individual springs. Velocity obtained from this mechanism is further connected to the derivative block to acquire the useful ambient acceleration. Finally, a force source is utilized to transfer this mechanical vibration to our main piezoelectric stack (PZT-5A), and because of linear time-variant mechanical vibrations, the alternating voltage is generated. Table 1 explains the parametric values used for the analysis and Figure 5 elaborates the complete numerical model of wind energy harvester based on the piezoelectric technique.

**Table 1.** Dimensions and properties of the proposed harvester.

Sr#	Parameters	Symbol	Unit	Values
1	Elastic Stiffness	$C_{33}$	$Nm^{-2}$	$11.09 \times 10^{10}$
2	Radius of Rotor	R	m	0.25
3	Swept Area	$A_s$	$m^2$	0.19
4	Number of Blades	-	-	3–5
5	VEM Stiffness	K	$Nm^{-1}$	10–40
6	Proof Mass	$m_p$	kg	0.5
7	Piezoelectric Charge Constant	$d_{33}$	C/N	$450 \times 10^{-12}$
8	Piezoelectric Coefficient	$g_{33}$	$m^2C^{-1}$	$24 \times 10^{-3}$
9	Permittivity	$\epsilon_{33}$	$Fm^{-1}$	$706 \times 10^{-11}$
10	Density	$\rho$	$Kgm^{-3}$	7750
11	Piezoelectric Stack’s Length	$L_p$	mm	10
12	Piezoelectric Stack’s Width	$w_p$	mm	20
13	Piezoelectric Stack’s Thickness	$t_p$	mm	0.5–4



**Figure 5.** Complete model of piezoelectric wind energy harvester on SIMSCAPE.

After it, the generated alternative voltage is interfaced with the electrical circuit, which contains a full-bridge rectifier to acquire the pulsating DC output of the energy harvester as shown in Figure 5. Additionally, the filter capacitor is connected in parallel with the resistive load to remove the undesirable frequencies (AC-Part) of the signal.

Numerical analysis of the proposed model is used to observe the effects of input variables such as wind speed, rotor angular velocity, resistive load, number of rotor-blades, PZT thickness, and stiffness on the electrical output of the energy harvester. And it is contemplated that wind speed has square and cubic relationships to the output voltage and power, respectively. In contrast, a non-linear relationship is observed between the number of blades of the rotor and harvested energy. Since air is the main working fluid in wind energy harvesters, so for a fluid with density ( $\rho$ ) flowing through the rotor of cross-sectional area ( $A$ ), the mass flow rate is given in Equation (12).

$$\dot{m} = \rho Av \tag{12}$$

Therefore, the thrust force produced in this way is equal to the time rate of change of linear momentum, which gives us the average force due to the motion of air particles as given in Equation (13). Consequently, it is found that the amplitude of alternative mechanical vibration is having a direct relationship to the square of the wind speed as given in Equation (14).

$$F = \frac{\Delta p}{t} = \frac{mv}{t} = \dot{m}v \quad (13)$$

$$F_{AVG} = \frac{\rho Av^2}{2} \quad (14)$$

Additionally, the thrust force in the piezoelectric energy harvesters is directly proportional to the output voltage. Therefore, by theoretical and numerical interpretations, it is observed that the output voltage is directly proportional to the square of the wind speed.

#### 4. Optimization Strategy for the Proposed Energy Harvester

In the recent past, several improvements have been made in the designs of energy scavengers to improve the electrical production capability of energy systems. Besides that, certain limitations have also been observed in the parametric values of those factors that are likely to influence the output response of energy harvesters. Additionally, it is completely unpredictable to determine the cumulative effect of input variables on the harvested electrical energy. Therefore, researchers have been trying to implement the optimization strategies on the recorded data to predict the maximum output and determine the critical values of the independent variables [48,49]. In this work, the optimization strategy is based on the statistical analysis that is utilized to correlate different variables of the proposed energy harvester. The objective function of the statistical model is to maximize the response of the energy harvester within predefined limits of input variables. Additionally, this optimization strategy is also used in determining the most influenced input factors with their optimum levels to enhance the solidity, effectiveness, and efficiency of the proposed energy harvester. Therefore, in this research work, a full factorial DOE is used to acquire optimum values of those input parameters that significantly affect the stable response of the energy harvester. Furthermore, the results of this experiment have been satisfied graphically by Pareto chart and contour plots. Figure 6 explains the complete workflow for evaluating the optimization strategy based on the factorial DOE.

##### *Factorial Design of Experiment*

A factorial design is a statistical tool that comprises several input factors with their levels to investigate the effect of each factor's level on the output of a certain system. This type of statistical model is further categorized as, full factorial DOE and fractional factorial DOE. Both approaches can detect the mutual interaction between independent variables; however, fractional factorial is preferable when the number of independent factors is greater than five in an experiment. Therefore, in this research work, the full factorial design of the experiment is implemented on MINITAB 18.0 to observe the effects of PZT thickness, stiffness of VEM, wind speed, and rotor blades on the electrical output of the energy harvester. Table 2 describes the levels of the input parameters and the total number of experimental runs required to complete this analysis are 16.

**Table 2.** Input variables of proposed energy harvester used in DOE.

Independent Factors	Unit	Low Level	High Level
Wind Speed	ms <sup>-1</sup>	5.5	8.5
Piezoelectric Thickness	mm	1.5	3.0
Stiffness of VEM	Nm <sup>-1</sup>	30	40
Number of Blades	-	3	4

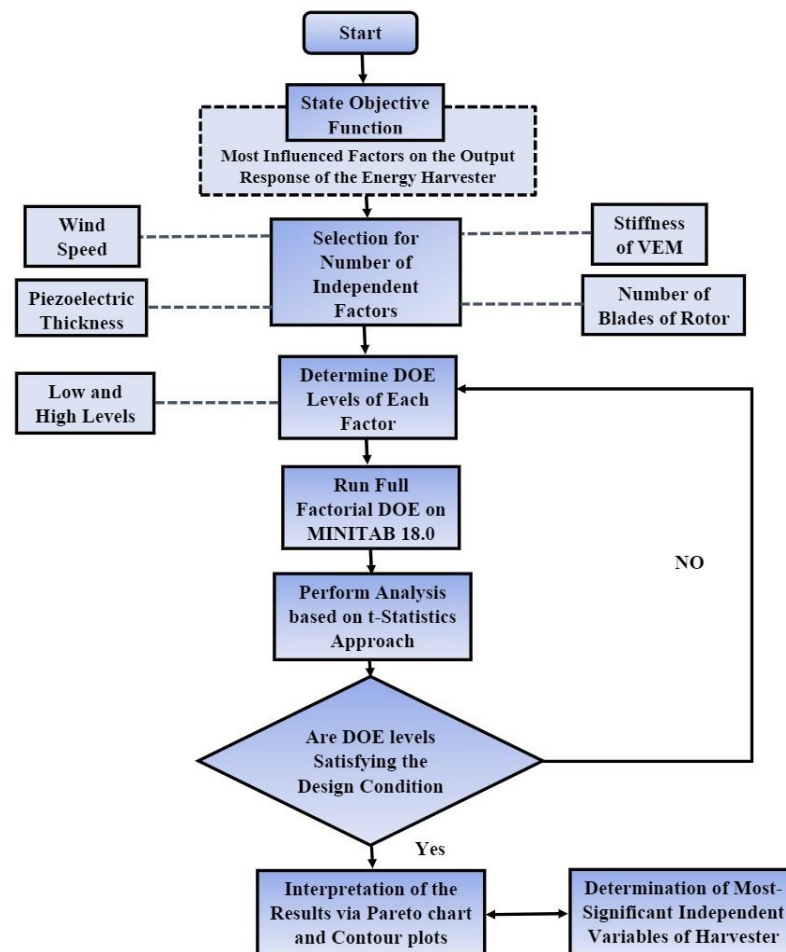


Figure 6. Optimization strategy based on full-factorial DOE.

## 5. Results and Discussions

In this section, the results of simulation and optimization have been discussed to analyze the performance of the proposed piezoelectric wind energy harvester.

### 5.1. Outcomes of Simulation

In this research work, wind speed is considered as the average of up-stream and down-stream wind velocities. Figures 7 and 8 show the response of the energy harvester in the form of output voltage (AC, DC), current, and power with the slight variation in the wind speed ranging from  $1.5 \text{ ms}^{-1}$  to  $14 \text{ ms}^{-1}$ . This response of wind-PZT energy harvester is observed at the constant values of stiffness ( $40 \text{ Nm}^{-1}$ ) and resistive load ( $50 \Omega$ ). Due to an increase in wind speed, the rotor of the windmill produces more rotational motion which will increase the amount of alternative mechanical vibrations obtained from the RLC mechanism. Therefore, the trendlines of Figure 7 show that the minimum speed at which the harvester produces sufficient energy is  $1.5 \text{ ms}^{-1}$ , known as the cut-in speed of the energy harvester. Furthermore, it can also be observed that the wind speed has square and cubic relationships with the output voltage and power of the energy harvester respectively as shown in Figures 7 and 8. Additionally, this analysis is accomplished through different trials based on the PZT thickness values of 2 mm, 4 mm, and 6 mm. It is found that PZT thickness has a positive linear impact on the response of wind energy harvester, which means that both output voltage and power will be increased with the values of PZT thickness.

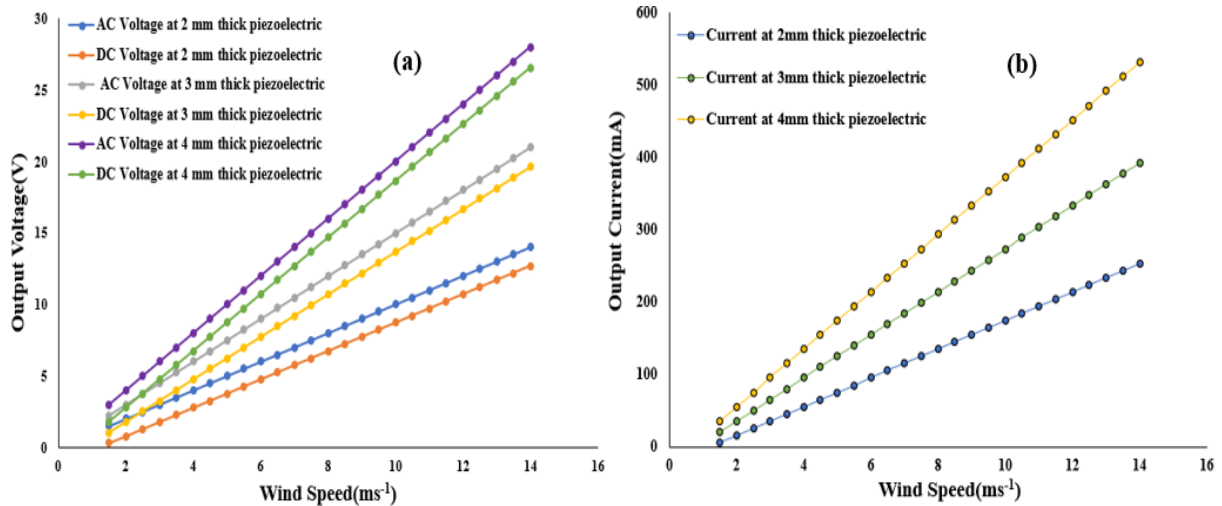


Figure 7. Electrical output of harvester via wind speed. (a) Output voltage, (b) Output current.

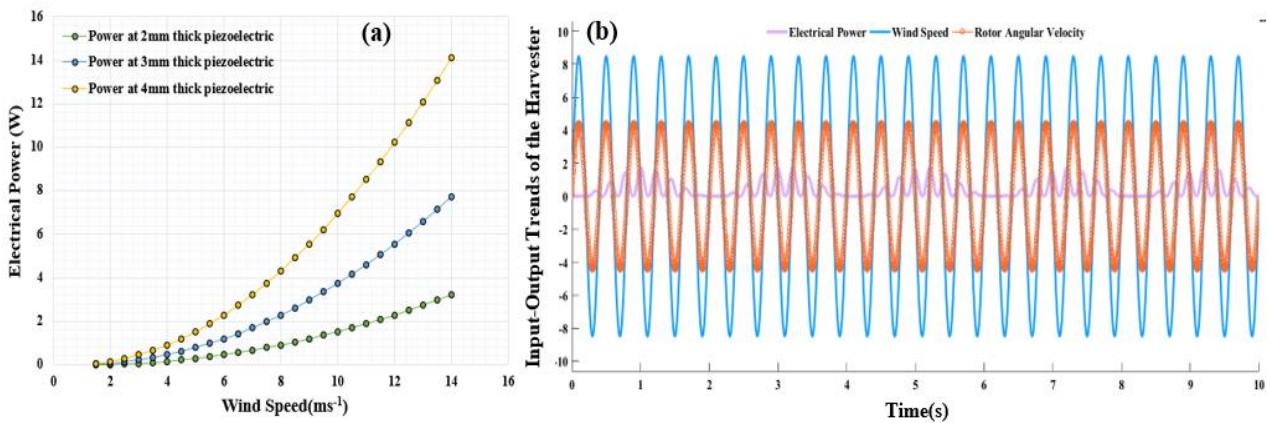


Figure 8. The response of the harvester. (a) Electrical power via wind speed, (b) Time varying trends of the harvester.

Results show that that the rated wind speed of this harvester fluctuates between  $1.5 \text{ ms}^{-1}$  to  $14 \text{ ms}^{-1}$  and Figure 8b shows the time-varying response in which the harvester produces a maximum output power of 1.8 W due to the dynamic input of wind speed. Additionally, it is also observed that under the specific condition of the input parameters, the electrical power is changed from 0.1705 to 1.757 W. One of the key reasons for this fluctuation is due to the external turbulences such as air pressure or temperature and air drag. Due to these reasons, average wind speed has been considered in the further analysis of the harvester to visualize the influence of piezoelectric transduction in harvesting wind energy.

It is evident that aerodynamic efficiency, being an important design factor for wind energy scavenging systems, is highly dependent on the rotor angular velocity. This angular velocity is affected by various factors such as the number of blades, rotor swept area, and wind speed. Therefore, the response of the energy harvester is analyzed and measured under different values of rotor angular velocity. On the contrary, the number of blades and PZT thickness are set to be 3 and 3 mm respectively. Figure 9 shows the measurement of different forms of output voltage and current with a slight variation in the rotor velocity ranging from  $0.7$  to  $7.5 \text{ rads}^{-1}$ . It is observed that due to an increase in rotor angular velocity, the response of the energy harvester increases. When air particles move across the circular plane created by the number of blades, the thrust force is developed which in turn forces the rotor to produce some rotational motion. Since rotor velocity is directly related to wind speed, therefore, due to an increase in wind speed, the rotor rotates with higher angular velocity up to a certain limit known as the cut-out speed of the harvester.

Consequently, mechanical vibration on PZT-Stack increases with rotor angular velocity, which in turn enhances the output response of the energy harvester as shown in Figure 9.

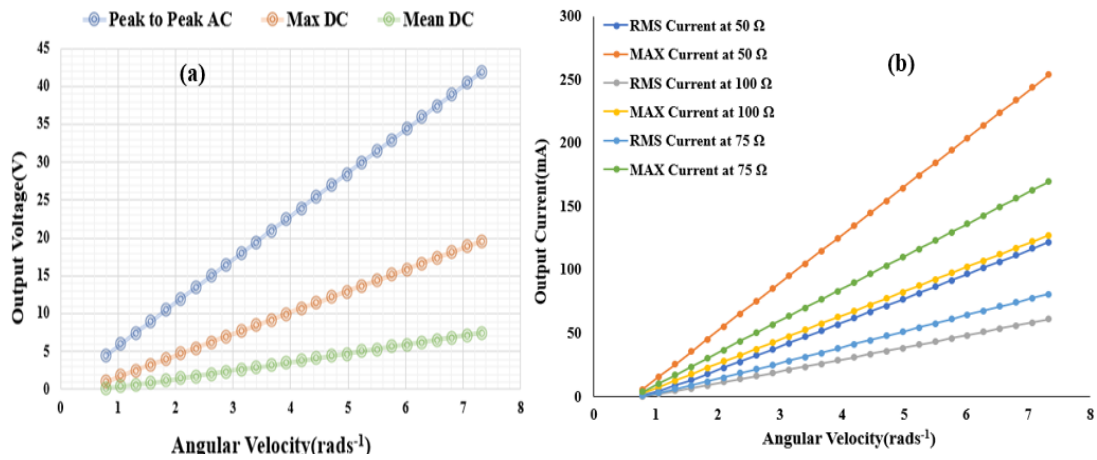


Figure 9. The response of energy harvester via angular velocity of rotor. (a) Output voltage, (b) Output current.

Additionally, three variant resistive loads (50, 75, and 100 Ω) are also included to analyze the electrical behavior of the piezoelectric wind energy harvester. It is found that resistance has a negative linear relationship with the electrical power and current, satisfying the principle of power dissipation as shown in Figure 10a. Furthermore, Figure 10b elaborates the time-varying response of the proposed harvester from where it has been contemplated that at an average wind speed of  $8.5 \text{ ms}^{-1}$ , and for three blades, the rotor of the windmill rotates with an optimal velocity of  $4.45 \text{ rads}^{-1}$ .

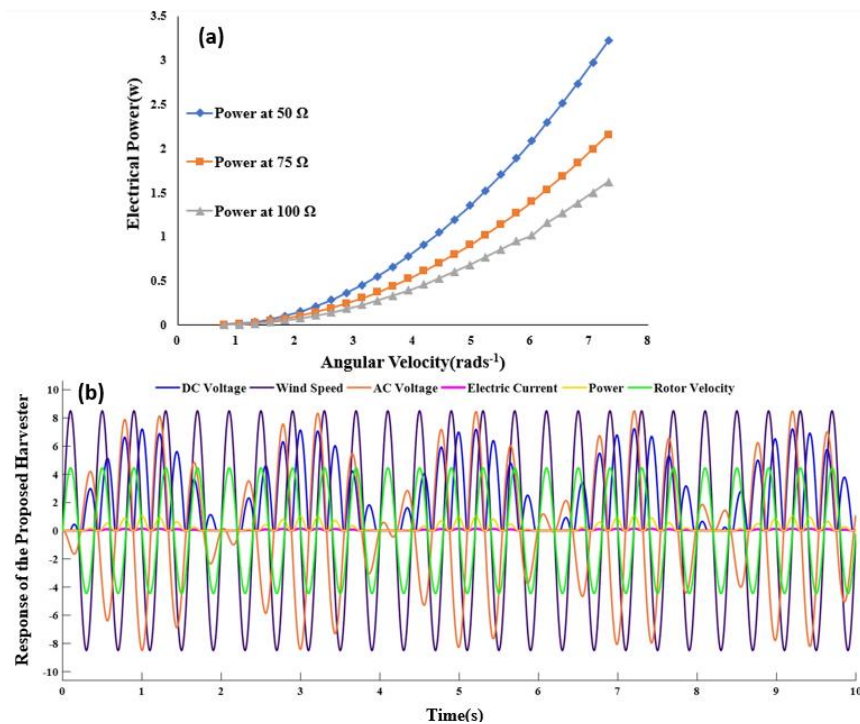


Figure 10. Output response. (a) Electrical power via angular velocity, (b) Dynamic input-output of the harvester.

The energy harvesting system based on the piezoelectric technique utilizes a direct piezoelectric effect to produce a useful electrical output. The internal characteristics of a PZT material such as width, length, and thickness play a crucial role in generating the

maximum output response from a typical energy harvester. Hence the design of the wind energy harvester is simulated by varying the thickness of PZT from 1 mm to 6 mm under the constant values of length and width of PZT-Stack. According to the theory of piezoelectric materials, thicker materials are capable to produce more separation of symmetric charges as compared to thinner materials. Therefore, a direct linear relationship between thickness and response of the proposed harvester has been observed as shown in Figures 11 and 12a. Additionally, the number of rotor-blades are also varied from three to five to check the solidity of a wind piezoelectric energy harvester and it can be noticed that a design with three number of blades is capable to produce sufficient electrical power. A harvester with a greater number of blades will automatically increase the density and swept area of the rotor. Therefore, according to the principle of continuity, a greater number of blades will try to reduce the translational velocity. Consequently, it is likely to say that rotor with three blades will produce more alternative vibration for PZT-Stack, and effectively increases the output response of the proposed energy harvester.

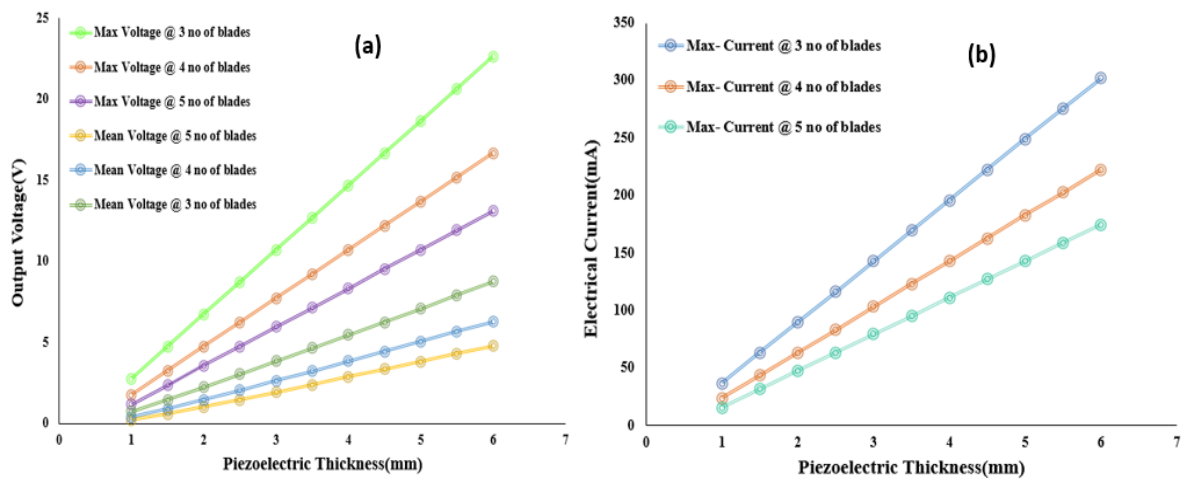


Figure 11. Measurement of output response of harvester via PZT thickness. (a) Output voltage, (b) Output current.

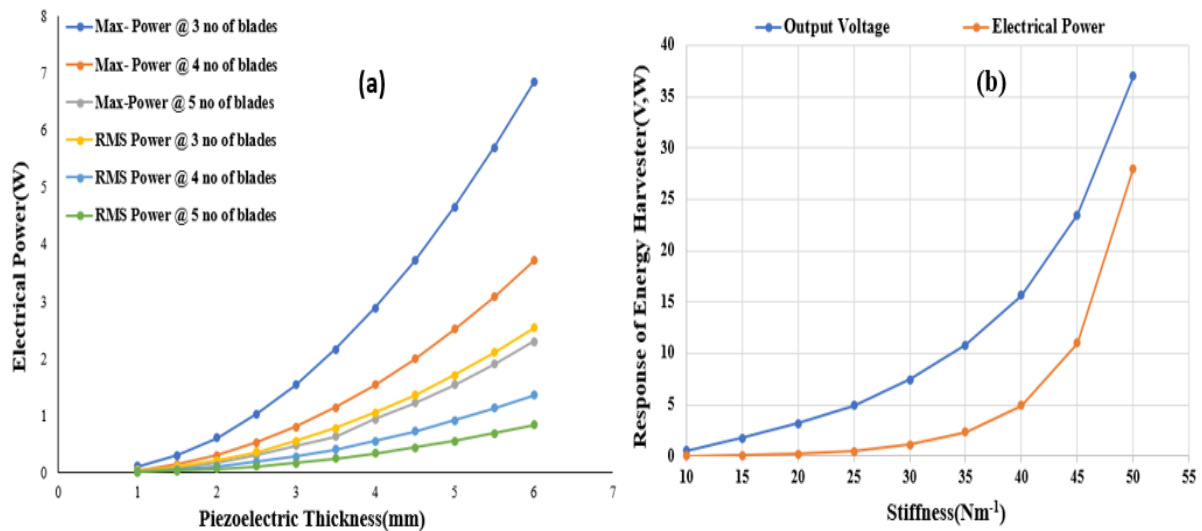


Figure 12. Response of harvester via. (a) Piezoelectric thickness, (b) Stiffness of VEM.

The output response of the energy harvester is highly dependent on the VEM which consists of a parallel combination of Hookean springs with a proof mass being attached to displace the mechanical vibration. Therefore, both output voltage and power are measured by varying the VEM-Stiffness values ranging from 10 Nm<sup>-1</sup> to 45 Nm<sup>-1</sup>. The wind speed, PZT thickness, and resistive load are set to be 8.5 ms<sup>-1</sup>, 4 mm, and 50 Ω respectively. The

trendlines of Figure 12b reveal that by increasing the stiffness, the amplitude of mechanical vibrations on PZT-Stack increases; consequently, it will enhance the output response of wind piezoelectric energy harvesters. Figure 12b also shows that after the stiffness value of  $40 \text{ Nm}^{-1}$ , the response of the harvester increases exponentially which is satisfying the theoretical analysis of the harvester; therefore, this value is considered as an optimal VEM-Stiffness for the proposed energy harvester.

### 5.2. Outcomes of Optimization Strategy

In the optimization strategies, t-statistics, along with the  $p$ -value approach have been widely used to interpret the results of the full factorial analysis. The main purpose of this statistical interpretation is to determine the best possible combination of input factor levels that would help us in generating the optimum electrical response from the proposed energy harvester. Interestingly, for a typical system with known input variables, the  $p$ -values of statistically significant factors will always be less than the predefined significance level ( $\alpha$ ). Therefore, the present statistical analysis is performed at a confidence interval of 95%. Consequently, the  $p$ -value of each input factor must be less than the level of significance ( $\alpha = 0.05$ ) to satisfy the results of the proposed energy harvester. Table 3 shows that PZT thickness ( $t = 8.29$ ,  $p = 0.001$ ), stiffness of VEM ( $t = 8.01$ ,  $p = 0.002$ ), and wind speed ( $t = 5.33$ ,  $p = 0.004$ ) are the three most significant input variables in producing the optimum response of energy harvester. Additionally, it is also observed that both PZT thickness and stiffness of VEM are highly correlated; therefore, values of both these factors should be carefully chosen to develop a robust piezoelectric wind energy harvester.

**Table 3.** Input variables of proposed energy harvester used in DOE.

Terms	Coefficient	SE Coeff.	$t$ -Value	$p$ -Value
Wind-Speed	1.110	0.208	5.33	0.004
Piezoelectric Thickness	1.727	0.208	8.29	0.001
Stiffness of VEM	1.668	0.208	8.01	0.002
Number of blades	−0.740	0.208	−3.55	0.005
Piezoelectric Thickness * Stiffness of VEM	0.556	0.208	2.67	0.023

\* Represents the interaction between parameters.

### Pareto and Contour Charts for Dominant Factors

A graphical representation that contains bar charts and a reference line to observe the effect of each input factor on the response of a system is known as a Pareto chart. In this research work, a Pareto chart is implemented on the standardized absolute values of all the input variables of the energy harvester. It is interesting to note that, reference line in the graph is highly dependent on the level of significance which is 0.05; therefore, independent variables whose bars will cross this reference line, are statistically significant. Consequently, Figure 13 shows that piezoelectric thickness and VEM stiffness are the two most dominant factors whose effect compared to the remaining variables is greater on the output response of piezoelectric wind energy harvester.

Furthermore, in this proposed design of energy harvester, a highly effective correlation is present between the two significant variables (PZT thickness, stiffness of VEM), as shown in Figure 13, satisfying the outcomes of simulation and t-statistics. Finally, contour plots are utilized to represent the graphical variation of the output voltage in response to the dominant input variables of the proposed energy harvester as shown in Figure 14. It is observed that the electrical response of the harvester becomes maximum at optimum values of VEM stiffness ( $40 \text{ Nm}^{-1}$ ), rotor-blades (3), and PZT thickness (3 mm).

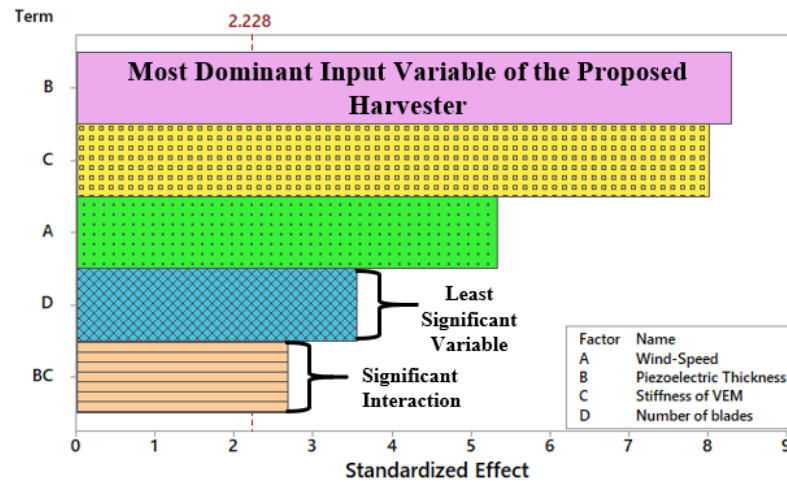


Figure 13. Selection of dominant input factors via Pareto chart.

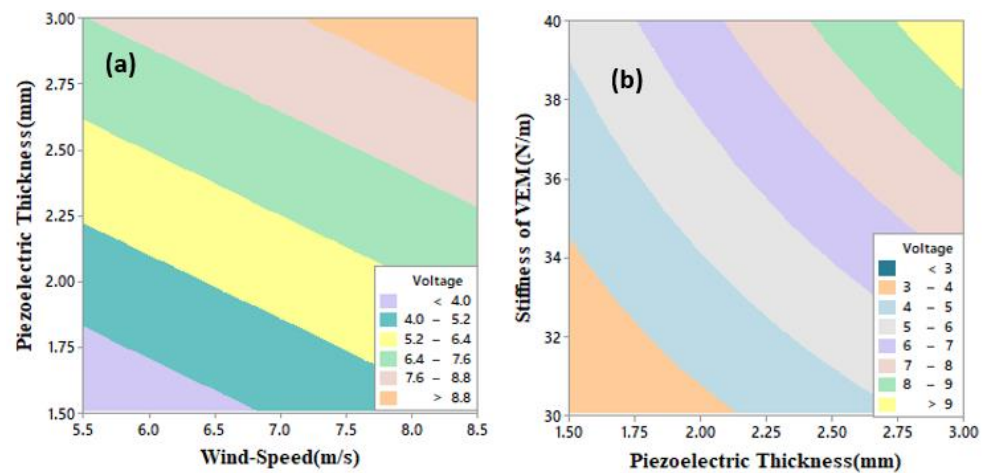


Figure 14. Variation of output voltage in response to dominant factors. (a) Wind Speed-Piezoelectric Thickness, (b) Piezoelectric Thickness-Stiffness of VEM.

5.3. A State of the Art-Comparison

In this section, a state-of-the-art comparison between piezoelectric wind energy harvesters is elaborated to highlight the significance of the proposed harvester. In a wind energy harvester based on the piezoelectric technique, the volume of the piezoelectric material plays a prominent role in generating stable electrical energy. Therefore, comparative analysis between different articles is developed by analyzing the electrical power concerning the piezoelectric dimensions. Furthermore, Table 4 shows a detailed set of electrical measurements in the form of cut-in speed, piezoelectric dimensions, and the used approach.

Table 4. Comparison of wind energy harvesters based on the piezoelectric technique.

References	Authors	Publication Year	Approach	Piezoelectric Dimensions	Cut-In Speed	Output Power
[25]	Wu. N et.al.	2013	Analytical	$0.12 \times 0.15 \times 0.0125 \text{ m}^3$	-	1.02 W @ $9 \text{ ms}^{-1}$
[50]	Zhao. L et.al.	2013	Analytical	$61 \times 30 \times 0.5 \text{ mm}^3$	$\sim 2.1 \text{ ms}^{-1}$	40 mW @ $14 \text{ ms}^{-1}$
[28]	Zhou. S et.al.	2019	Analytical and Experimental	-	$1.3 \text{ ms}^{-1}$	1.2 mW @ $2.2 \text{ ms}^{-1}$
[51]	Wei et.al.	2020	Analytical and Experimental	$46 \times 10 \times 1 \text{ mm}^3$	$2 \text{ ms}^{-1}$	$35.6 \mu\text{W}$ @ $5.45 \text{ ms}^{-1}$
[52]	Wang. K et.al.	2020	Analytical and Numerical	$100 \times 30 \times 0.3 \text{ mm}^3$	$6 \text{ ms}^{-1}$	0.12 W @ $17\text{--}18 \text{ ms}^{-1}$
[53]	Sitharthan. R et.al.	2021	Experimental	$0.00234 \text{ m}^3$	$< 3 \text{ ms}^{-1}$	2.6 W @ $9\text{--}11 \text{ ms}^{-1}$
[54]	Shi.T et.al.	2021	Experimental	-	$\sim 2.1 \text{ ms}^{-1}$	3 mW @ $4 \text{ ms}^{-1}$
[55]	Silva et.al.	2021	Numerical and Experimental	$12.9 \text{ mm}^3$	-	2.06 mW
Proposed work	Sheeraz et.al.	-	Numerical	$10 \times 20 \times 3 \text{ mm}^3$	$\sim 1.5 \text{ ms}^{-1}$	2.622 W @ $8.5 \text{ ms}^{-1}$

The most recent publications also enlighten the fluctuations in the cut-in speed via the length, width, and thickness of the piezoelectric material. Due to these reasons, another comparison in the form of power density has been developed to interpret the significance of the harvested electrical power as shown in Figure 15. It is concluded that power density obtained for this harvester at a specific case of piezoelectric dimension is in well-agreement and typically higher as compared to the values reported in the literature. Results also enlightened that the proposed piezoelectric wind energy harvester can produce a power density of  $0.25 \text{ mW/mm}^3$  at 1.5 mm piezoelectric thickness.

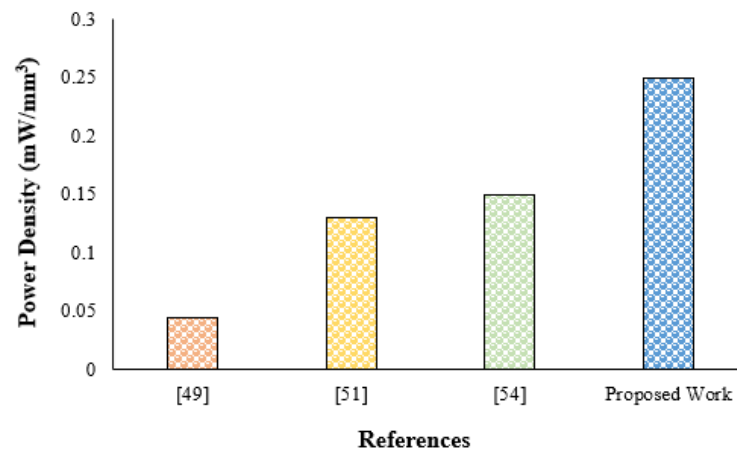


Figure 15. Comparison of harvested energy in terms of power density.

## 6. Conclusions

Energy harvesters are getting popular to fill the energy gap by utilizing the available natural resources. Therefore, in this research work, a cost-effective wind energy harvester based on the piezoelectric technique was modeled, numerically simulated, and optimized to obtain electrical energy even at low wind speeds. The proposed harvester consists of a windmill for acquiring mechanical power (rotational motion) due to the wind motion. However, for the piezoelectric materials, it is necessary to have linear alternative mechanical vibrations; therefore, a rotary to linear converter (RLC) was used to generate the vibrations for the piezoelectric stack (PZT-5A). It was noticed that the amplitude of mechanical vibration is not enough to drive the piezoelectric materials into a polarization state. Hence, a vibration enhancement mechanism (VEM) consisted of a combination of Hookean springs, and a proof mass has been utilized to increase the amount of thrust force for producing sufficient electrical energy. An analytical model of wind energy harvester was presented by including the mechanical-electrical transduction of piezoelectric materials. MATLAB toolbox SIMSCAPE was used to numerically simulate the proposed harvester under the various conditions of input parameters, and it was observed that the cut-in speed of the harvester is  $1.5 \text{ ms}^{-1}$ . Additionally, the response of the wind harvester was investigated by varying wind speed, rotor angular velocity, piezoelectric thickness, and VEM stiffness to observe the various parametric relationships of the harvester. It was noticed that the electrical efficiency of the harvester is highly dependent on the stiffness of the vibration enhancement mechanism (VEM). Finally, the full factorial design of the experiment (DOE) was implemented to statistically optimize the input parameters of the proposed wind energy harvester. The optimization results are in good agreement with the simulation, and literature outcomes. Therefore, based on the outcomes of the proposed work, it is recommended to develop and utilize this low-cost, efficient, and robust proposed harvester to power the sensor nodes in wireless networking.

**Author Contributions:** Conceptualization, M.A.S., M.S.M. and Z.B.; methodology, M.A.S., H.E. and M.S.M.; software, M.A.S.; formal analysis, I.A., Z.B.; investigation, M.A.S., M.S.M. and K.R.; resources, H.E., M.S.M., K.R. and Z.B.; writing—original draft preparation, M.A.S., writing—review and editing,

H.E., P.G., M.S.M., K.R and M.E.; visualization, M.A.S., H.E., M.S.M. and K.R.; supervision, M.S.M. and K.R.; project administration, M.S.M. and K.R.; funding acquisition, H.E., P.G. and M.E. All authors have read and agreed to the published version of the manuscript.

**Funding:** This research received no external funding.

**Institutional Review Board Statement:** Not applicable.

**Informed Consent Statement:** Not applicable.

**Data Availability Statement:** Not applicable.

**Conflicts of Interest:** The authors declare no conflict of interest.

## Nomenclature

A	Rotor Cross Sectional Area
$C_{33}$	Elastic Stiffness
$C_p$	Piezoelectric Capacitance
$d_{33}$	Piezoelectric Coefficient
$E_{33}$	Piezoelectric Constant
$F_p$	Equivalent Piezoelectric force
$K_b$	Stiffness of VEM
$K_p$	Stiffness of Piezoelectric layer
$L_p$	Piezoelectric Stack's Length
$L_b$	Length of rotor blade
$t_p$	Thickness of Piezoelectric Stack
$w_p$	Piezoelectric Stack's Width
Z	Distance between slider and slotted rod
$Z_e$	Equivalent Displacement
$\eta_m$	Magnifying Ratio
A	Level of Significance

## Acronyms

DOE	Design of Experiment
DOF	Degree of Freedom
FSI	Fluid Structure Interaction
LCO	Limit Cycle Oscillation
MATLAB	Matrix Laboratory
PZT	Lead Zirconate Titanate
RLC	Rotary to linear Converter
VEM	Vibration Enhancement Mechanism

## References

1. Zeadally, S.; Shaikh, F.K.; Talpur, A.; Sheng, Q.Z. Design architectures for energy harvesting in the Internet of Things. *Renew. Sustain. Energy Rev.* **2020**, *128*, 109901. [[CrossRef](#)]
2. Wei, C.; Jing, X. A comprehensive review on vibration energy harvesting: Modelling and realization. *Renew. Sustain. Energy Rev.* **2017**, *74*, 1–18. [[CrossRef](#)]
3. Sarker, M.R.; Julai, S.; Sabri, M.F.M.; Said, S.M.; Islam, M.M.; Tahir, M. Review of piezoelectric energy harvesting system and application of optimization techniques to enhance the performance of the harvesting system. *Sens. Actuators A Phys.* **2019**, *300*, 111634. [[CrossRef](#)]
4. Ahmad, I.; Ur Rehman, M.M.; Khan, M.; Abbas, A.; Ishfaq, S.; Malik, S. Flow-based electromagnetic-type energy harvester using microplanar coil for IoT sensors application. *Int. J. Energy Res.* **2019**, *43*, 5384–5391. [[CrossRef](#)]
5. Shakeel, M.; Rehman, K.; Ahmad, S.; Amin, M.; Iqbal, N.; Khan, A. A low-cost printed organic thermoelectric generator for low-temperature energy harvesting. *Renew. Energy* **2021**, *167*, 853–860. [[CrossRef](#)]
6. Watson, S.; Moro, A.; Reis, V.; Baniotopoulos, C.; Barth, S.; Bartoli, G.; Bauer, F.; Boelman, E.; Bosse, D.; Cherubini, A.; et al. Future emerging technologies in the wind power sector: A European perspective. *Renew. Sustain. Energy Rev.* **2019**, *113*, 109270. [[CrossRef](#)]
7. Liu, Z.; Zhang, L. A review of failure modes, condition monitoring and fault diagnosis methods for large-scale wind turbine bearings. *Meas. J. Int. Meas. Confed.* **2020**, *149*, 107002. [[CrossRef](#)]
8. Wang, T.; Han, Q.; Chu, F.; Feng, Z. Vibration based condition monitoring and fault diagnosis of wind turbine planetary gearbox: A review. *Mech. Syst. Signal Process.* **2019**, *126*, 662–685. [[CrossRef](#)]

9. Paulsamy, S. Reduction of cogging torque in dual rotor permanent magnet generator for direct coupled wind energy systems. *Sci. World J.* **2014**, *2014*. [[CrossRef](#)]
10. Zhang, L.; Guo, Y.; Wang, J.; Huang, X.; Wei, X.; Liu, W. Structural failure test of a 52.5 m wind turbine blade under combined loading. *Eng. Fail. Anal.* **2019**, *103*, 286–293. [[CrossRef](#)]
11. Mishnaevsky, L. Repair of wind turbine blades: Review of methods and related computational mechanics problems. *Renew. Energy* **2019**, *140*, 828–839. [[CrossRef](#)]
12. Ilbahar, E.; Cebi, S.; Kahraman, C. A state-of-the-art review on multi-attribute renewable energy decision making. *Energy Strateg. Rev.* **2019**, *25*, 18–33. [[CrossRef](#)]
13. Shahid, M.; Ullah, K.; Imran, K.; Mahmood, I.; Mahmood, A. Electricity supply pathways based on renewable resources: A sustainable energy future for Pakistan. *J. Clean. Prod.* **2020**, *263*, 121511. [[CrossRef](#)]
14. Zhao, L.; Yang, Y. An impact-based broadband aeroelastic energy harvester for concurrent wind and base vibration energy harvesting. *Appl. Energy* **2018**, *212*, 233–243. [[CrossRef](#)]
15. Saadon, S.; Sidek, O. A review of vibration-based MEMS piezoelectric energy harvesters. *Energy Convers. Manag.* **2011**, *52*, 500–504. [[CrossRef](#)]
16. Briscoe, J.; Dunn, S. Piezoelectric nanogenerators—A review of nanostructured piezoelectric energy harvesters. *Nano Energy* **2014**, *14*, 15–29. [[CrossRef](#)]
17. Elahi, H.; Eugeni, M.; Gaudenzi, P. A review on mechanisms for piezoelectric-based energy harvesters. *Energies* **2018**, *11*, 1850. [[CrossRef](#)]
18. Covaci, C.; Gontean, A. Piezoelectric energy harvesting solutions: A review. *Sensors* **2020**, *20*, 3512. [[CrossRef](#)] [[PubMed](#)]
19. Elahi, H.; Eugeni, M.; Gaudenzi, P.; Qayyum, F.; Swati, R.F.; Khan, H.M. Response of piezoelectric materials on thermomechanical shocking and electrical shocking for aerospace applications. *Microsyst. Technol.* **2018**, *24*, 3791–3798. [[CrossRef](#)]
20. Ahmad, I.; Hassan, A.; Anjum, M.U.; Malik, S.; Ali, T. Ambient Acoustic Energy Harvesting using Two Connected Resonators with Piezoelement for Wireless Distributed Sensor Network. *Acoust. Phys.* **2019**, *65*, 471–477. [[CrossRef](#)]
21. Pradeesh, E.L.; Udhayakumar, S. Effect of placement of piezoelectric material and proof mass on the performance of piezoelectric energy harvester. *Mech. Syst. Signal Process.* **2019**, *130*, 664–676. [[CrossRef](#)]
22. Karafi, M.R.; Khorasani, F. Evaluation of mechanical and electric power losses in a typical piezoelectric ultrasonic transducer. *Sensors Actuators A Phys.* **2019**, *288*, 156–164. [[CrossRef](#)]
23. Orrego, S.; Shoele, K.; Ruas, A.; Doran, K.; Caggiano, B.; Mittal, R.; Kang, S.H. Harvesting ambient wind energy with an inverted piezoelectric flag. *Appl. Energy* **2017**, *194*, 212–222. [[CrossRef](#)]
24. Sheeraz, M.A.; Butt, Z.; Khan, A.M.; Mehmood, S.; Ali, A.; Azeem, M.; Nasir, A.; Imtiaz, T. Design and Optimization of Piezoelectric Transducer (PZT-5H Stack). *J. Electron. Mater.* **2019**, *48*, 6487–6502. [[CrossRef](#)]
25. Wu, N.; Wang, Q.; Xie, X. Wind energy harvesting with a piezoelectric harvester. *Smart Mater. Struct.* **2013**, *22*. [[CrossRef](#)]
26. Priya, S. Modeling of electric energy harvesting using piezoelectric windmill. *Appl. Phys. Lett.* **2005**, *87*, 1–3. [[CrossRef](#)]
27. Elahi, H.; Eugeni, M.; Gaudenzi, P. Design and performance evaluation of a piezoelectric aeroelastic energy harvester based on the limit cycle oscillation phenomenon. *Acta Astronaut.* **2019**, *157*, 233–240. [[CrossRef](#)]
28. Wang, J.; Zhou, S.; Zhang, Z.; Yurchenko, D. High-performance piezoelectric wind energy harvester with Y-shaped attachments. *Energy Convers. Manag.* **2019**, *181*, 645–652. [[CrossRef](#)]
29. Zhang, L.B.; Abdelkefi, A.; Dai, H.L.; Naseer, R.; Wang, L. Design and experimental analysis of broadband energy harvesting from vortex-induced vibrations. *J. Sound Vib.* **2017**, *408*, 210–219. [[CrossRef](#)]
30. Yu, H.; Zhang, M. Effects of side ratio on energy harvesting from transverse galloping of a rectangular cylinder. *Energy* **2021**, 120420. [[CrossRef](#)]
31. Caracoglia, L. Modeling the coupled electro-mechanical response of a torsional-flutter-based wind harvester with a focus on energy efficiency examination. *J. Wind Eng. Ind. Aerodyn.* **2018**, *174*, 437–450. [[CrossRef](#)]
32. Elahi, H. The investigation on structural health monitoring of aerospace structures via piezoelectric aeroelastic energy harvesting. *Microsyst. Technol.* **2020**, 1–9. [[CrossRef](#)]
33. Elahi, H.; Munir, K.; Eugeni, M.; Atek, S.; Gaudenzi, P. Energy Harvesting towards Self-Powered IoT Devices. *Energies* **2020**, *13*, 5528. [[CrossRef](#)]
34. Elahi, H.; Eugeni, M.; Fune, F.; Lampani, L.; Mastroddi, F.; Paolo Romano, G.; Gaudenzi, P. Performance evaluation of a piezoelectric energy harvester based on flag-flutter. *Micromachines* **2020**, *11*, 933. [[CrossRef](#)] [[PubMed](#)]
35. Chawdhury, S.; Milani, D.; Morgenthal, G. Modeling of pulsating incoming flow using vortex particle methods to investigate the performance of flutter-based energy harvesters. *Comput. Struct.* **2018**, *209*, 130–149. [[CrossRef](#)]
36. Aquino, A.I.; Calautit, J.K.; Hughes, B.R. A Study on the Wind-Induced Flutter Energy Harvester (WIFEH) Integration into Buildings. *Energy Procedia* **2017**, *142*, 321–327. [[CrossRef](#)]
37. Eugeni, M.; Elahi, H.; Fune, F.; Lampani, L.; Mastroddi, F.; Romano, G.P.; Gaudenzi, P. Numerical and experimental investigation of piezoelectric energy harvester based on flag-flutter. *Aerosp. Sci. Technol.* **2020**, *97*, 105634. [[CrossRef](#)]
38. Elvin, N.G.; Elvin, A.A. The flutter response of a piezoelectrically damped cantilever pipe. *J. Intell. Mater. Syst. Struct.* **2009**, *20*, 2017–2026. [[CrossRef](#)]
39. Bae, J.S.; Inman, D.J. Aeroelastic characteristics of linear and nonlinear piezo-aeroelastic energy harvester. *J. Intell. Mater. Syst. Struct.* **2014**, *25*, 401–416. [[CrossRef](#)]

40. Kishore, R.A.; Vučković, D.; Priya, S. Ultra-low wind speed piezoelectric windmill. *Ferroelectrics* **2014**, *460*, 98–107. [[CrossRef](#)]
41. Hsieh, J.C.; Lin, D.T.W.; Lin, C.L. The development and optimization of an innovative piezoelectric energy harvester on the basis of vapor-induced vibrations. *Mech. Syst. Signal Process.* **2019**, *131*, 649–658. [[CrossRef](#)]
42. Lü, C.; Zhang, Y.; Zhang, H.; Zhang, Z.; Shen, M.; Chen, Y. Generalized optimization method for energy conversion and storage efficiency of nanoscale flexible piezoelectric energy harvesters. *Energy Convers. Manag.* **2019**, *182*, 34–40. [[CrossRef](#)]
43. Schoeftner, J.; Buchberger, G. A contribution on the optimal design of a vibrating cantilever in a power harvesting application—Optimization of piezoelectric layer distributions in combination with advanced harvesting circuits. *Eng. Struct.* **2013**, *53*, 92–101. [[CrossRef](#)]
44. Merabet Boulouiha, H.; Khodja, M.; Rahiel, D.; Allali, A.; Kaddour, F.; Denäi, M. Power quality enhancement in electricity grids with wind energy using multicell converters and energy storage. *J. Renew. Sustain. Energy* **2019**, *11*. [[CrossRef](#)]
45. Morel, A.; Badel, A.; Grézaud, R.; Gasnier, P.; Despesse, G.; Pillonnet, G. Resistive and reactive loads' influences on highly coupled piezoelectric generators for wideband vibrations energy harvesting. *J. Intell. Mater. Syst. Struct.* **2019**, *30*, 386–399. [[CrossRef](#)]
46. Qian, F.; Xu, T.; Zuo, L. Design, optimization, modeling and testing of a piezoelectric footwear energy harvester. *Energy Convers. Manag.* **2018**, *171*, 1352–1364. [[CrossRef](#)]
47. Wang, Q. Energy harvesting from wind by a piezoelectric harvester. *Eng. Struct.* **2017**, *133*, 74–80. [[CrossRef](#)]
48. Tyagi, K.; Tyagi, K. A Comparative Analysis of Optimization Techniques. *Int. J. Comput. Appl.* **2015**, *131*, 6–12. [[CrossRef](#)]
49. Wang, X.; Li, L.; Palazoglu, A.; El-Farra, N.H.; Shah, N. Optimization and control of offshore wind systems with energy storage. *Energy Convers. Manag.* **2018**, *173*, 426–437. [[CrossRef](#)]
50. Zhao, L.; Tang, L.; Yang, Y. Comparison of modeling methods and parametric study for a piezoelectric wind energy harvester. *Smart Mater. Struct.* **2013**, *22*. [[CrossRef](#)]
51. Zhou, H.; Wei, K.; Liu, J. Enhanced performance of piezoelectric wind energy harvester by a curved plate. *Smart Mater. Struct.* **2020**, *28*. [[CrossRef](#)]
52. Wang, K.F.; Wang, B.L.; Gao, Y.; Zhou, J.Y. Nonlinear analysis of piezoelectric wind energy harvesters with different geometrical shapes. *Arch. Appl. Mech.* **2020**, *90*, 721–736. [[CrossRef](#)]
53. Sitharthan, R.; Yuvaraj, S.; Padmanabhan, S.; Holm-Nielsen, J.B.; Sujith, M.; Rajesh, M.; Prabaharan, N.; Vengatesan, K. Piezoelectric energy harvester converting wind aerodynamic energy into electrical energy for microelectronic application. *IET Renew. Power Gener.* **2021**. [[CrossRef](#)]
54. Shi, T.; Hu, G.; Zou, L.; Song, J.; Kwok, K.C.S. Performance of an omnidirectional piezoelectric wind energy harvester. *Wind Energy* **2021**, 1–13. [[CrossRef](#)]
55. Pauloe Silva, A.G.; Basílio Sobrinho, J.M.; da Rocha Souto, C.; Ries, A.; de Castro, A.C. Design, modelling and experimental analysis of a piezoelectric wind energy generator for low-power applications. *Sens. Actuators A Phys.* **2021**, *317*. [[CrossRef](#)]